Journal of the European Ceramic Society **10** (1992) 13–20

Superplastic Deformation of an Alumina–Zirconia Matrix Reinforced with SiC Whiskers

G. Bernard-Granger, R. Baddi,* R. Duclos‡ & J. Crampon

Laboratoire de Structure et Propriétés de l'Etat Solide, URA 234, Bât. C6, Université de Lille 1, 59655 Villeneuve d'Ascq Cédex, France

(Received 29 July 1991; revised version received 23 October 1991; accepted 24 October 1991)

Abstract

Alumina–zirconia ceramics reinforced with SiC whiskers have been superplastically deformed during compressive creep tests up to true strains near 90%. Deformation resulted mainly from diffusion mechanisms. The influence of whisker orientation relative to stress axis has been studied. It appeared that the angle between the whisker direction and the stress axis is not adequate to characterize the resultant creep rate. It is the direction of the matter flow relative to the whisker axis which seemed to be the preponderant criterion. Observations of porosity in highly strained specimens are in agreement with superplasticity models involving pores as a second phase.

SiC-Whisker verstärkte Aluminiumoxid–Zirkoniumoxid-Keramiken wurden in Kriechexperimenten unter Druckbeanspruchung superplastisch bis hin zu einer wahren Dehnung von etwa 90% verformt. Die Verformung wird hauptsächlich auf Diffusionsmechanismen zurückgeführt. Es wurde der Einfluß der Whisker-Orientierung relativ zur Beanspruchungsrichtung untersucht. Hierbei konnte gezeigt werden, daß der Winkel zwischen der Ausrichtung der Whisker und der Beanspruchungsrichtung nicht als Kriterium zur Beurteilung der Kriechgeschwindigkeit herangezogen werden kann. Vielmehr ist die Richtung des Materieflusses relativ zur Orientierung der Whisker das vorherrschende Kriterium. Beobachtungen bezüglich der Porosität hochverformter Proben sind in guter Übereinstimmung mit Modellen, die die Superplastizität in Materialien mit Poren als sekundärer Phase beschreiben.

Des céramiques à matrice alumine–zircone renforcée par des whiskers de SiC ont été déformées superplastiquement jusqu'à des taux proches de 90% au cours d'essais de fluage en compression. On a observé que la déformation résultait principalement de mécanismes de diffusion. On a étudié le rôle de l'orientation des whiskers par rapport à l'axe de compression. On montre en particulier que l'angle entre la direction du whisker et l'axe de compression n'est pas un critère suffisant pour caractériser la vitesse de fluage. C'est la direction des flux de matière par rapport à l'axe des whiskers qui semble être le critère prépondérant. La porosité observée dans des échantillons fortement déformés est en bon accord avec les modèles de superplasticité mettant en jeu des pores comme seconde phase.

1 Introduction

Superplasticity of single- or two-phase ceramics is now well demonstrated. In these materials, large superplastic strains can be achieved when grain sizes are small (typically finer than one micrometre) and grain growth as slow as possible.[1,2] In alumina polycrystals for example, the inherent grain growth prevents the possibility of obtaining very large strains;[3] this grain growth can be avoided by adding zirconia particles which make easier the observation of superplastic deformation in these composites, as was recently demonstrated.[4,5]

When a rigid phase, as SiC whiskers are, for example, is added to a superplastic matrix, the achievement of large strains requires that the deformation of the matrix is consistent with that of the hard phase to minimize the nucleation of voids in the composite. Very little work has been performed

* On leave from Université Mohamed 1er, Faculté des Sciences, Oujda, Morocco.
‡ To whom correspondence should be addressed.

Journal of the European Ceramic Society 0955-2219/92/$5.00 © 1992 Elsevier Science Publishers Ltd, England. Printed in Great Britain

from the mechanical and structural viewpoints, on the influence of such hard phases on the superplasticity properties of ceramic matrices.[6-8]

The purpose of this paper is to investigate the ability of alumina-based ceramics reinforced with SiC whiskers to be deformed up to large strains near 100% and the related microstructural development of the material. In a previous work[9] the mechanical behaviour of a similar composite material was studied between 1250 and 1450°C up to strains near 30%. The main results concerned the high creep activation energy, 800 to 900 kJ/mol, and the observation of a temperature-dependent threshold stress. That threshold stress, whose origin likely resulted from interface processes, could not be fully explained by existing deformation models taking into account grain boundary dislocations.[10,11] This paper deals with the influence on mechanical behaviour of whisker orientation relative to stress direction. This influence has been studied not only on the threshold stress, but, more generally, on the macroscopic behaviour of the composite and on microstructure development: grain size and shape, whisker-stress interaction, porosity nucleation and growth.

2 Experimental Procedure

A hot-pressed disc (diameter 80 mm, thickness 15 mm) of a mixture containing volume ratios of alumina, zirconia and silicon carbide whiskers equal to 65%, 10% and 25%, respectively, was supplied by Céramiques Techniques Desmarquest (Evreux, France). The fabrication process and the composite microstructure have already been described in detail elsewhere.[12] The density of the fully densified hot-pressed material was 4·01 g/cm^3 and the main impurities are given in Table 1. The grain sizes were approximately 1 μm for alumina phase, 0·5 μm for zirconia grains and 0·5 to 1 μm in diameter and up to 10 μm length for the whiskers. If no glassy grain boundary phase was detected in transmission electron microscopy (TEM) in this material, the occurrence of such a phase cannot be completely eliminated regarding the impurity content. Samples with the compression axis parallel or perpendicular to the hot-pressing direction (h-p.d.), designated as

Table 1. Impurity content of the composite

Impurity (*wt*%)	*MgO*	*CaO*	Fe_2O_3	TiO_2
	0·012	0·028	0·050	0·020

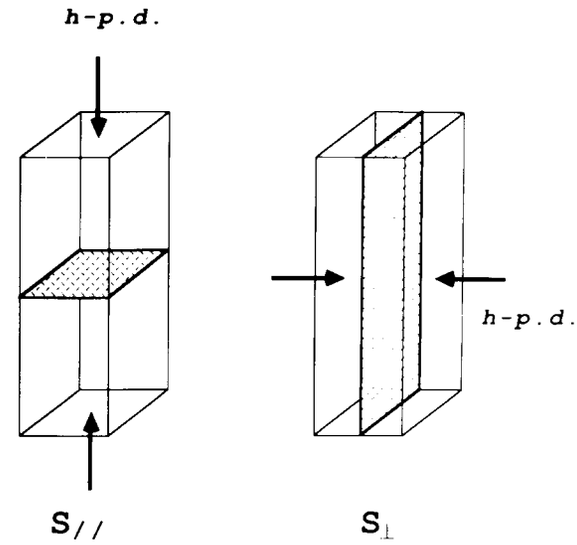

Fig. 1. Schematic drawing of S// and S⊥ specimens. The hot-pressing direction and a perpendicular plane containing the whiskers are represented.

S// and S⊥ respectively, were then cut in the disc (Fig. 1). The sample size was typically 3 mm × 3 mm × 8 mm. The structure of the composite was approximately homogeneous but not isotropic, almost all whiskers being confined in planes perpendicular to the pressing direction. Under these conditions the whisker orientation influence could be studied effectively, S// and S⊥ corresponding to whiskers lying in planes perpendicular or parallel to the compression axis respectively (Fig. 1). Compressive deformation tests were performed in air at 1350 and 1400°C up to strains near 90%. On average two or three samples were tested for each specific condition.

From each creep-tested sample, thin foils parallel and/or perpendicular to the compression axis were cut for TEM observations in order to account for microstructure development, especially for the effect of whiskers during deformation. The foils were first mechanically polished before the final stage of ion thinning. TEM observations were made at 200 kV.

3 Experimental Results

3.1 Mechanical study

From creep curves obtained at constant stress and presented in Fig. 2 as a plot of creep rate versus strain, it is apparent that creep rate of S⊥ samples was about three to five times faster than that of S// specimens for identical deformation conditions. This is the only difference that exists from the mechanical viewpoint between the two kinds of specimens. After a 20% strain, the creep rate became nearly constant whatever the final strain was, up to

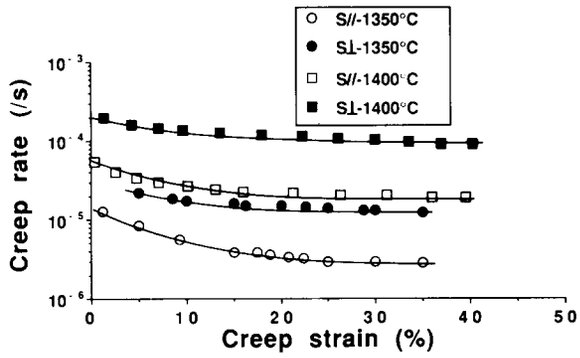

Fig. 2. Semi-logarithmic plot of creep rate versus true strain for S// and S⊥ specimens. Deformation conditions are indicated on the diagram. Stress: 50 MPa.

88%, and for a specific test condition the curves were reproducible.

The dependence of creep rate on the applied stress, characterized by the stress exponent n in the usually observed high-temperature deformation relationship:

$$\dot{\varepsilon} = \dot{\varepsilon}_0 \sigma^n \exp(-Q/kT) \qquad (1)$$

with $\dot{\varepsilon}_0$ a scaling parameter, σ the applied stress and Q the apparent activation energy, increased from 1·4 to 8 and more when stress decreased as shown in Fig. 3(a), in agreement with previous results.[9] A linear

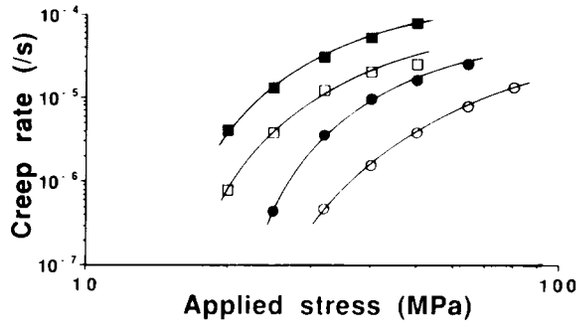

(a)

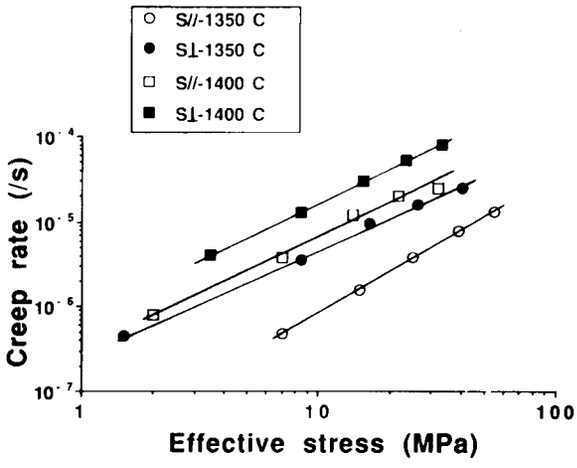

(b)

Fig. 3. Log–log plots of: (a) the creep rate versus the applied stress, (b) the creep rate versus the effective stress.

dependence of creep rate on the stress was obtained in a logarithmic plot only if a threshold stress σ_t was introduced in the above relation which was then written as:

$$\dot{\varepsilon} = \dot{\varepsilon}_e (\sigma - \sigma_t)^{n_e} \exp(-Q_e/kT) \qquad (2)$$

$\sigma - \sigma_t$ being the effective stress (Fig. 3(b)). The average value of the effective stress exponent n_e was equal to $1{\cdot}4 \pm 0{\cdot}3$, corresponding to threshold stresses equal to 25 and 18 MPa at 1350 and 1400°C respectively, insensitive to the specimen orientation and slightly lower than the values obtained previously.[9]

From temperature changes the creep activation energy Q_e was determined; it ranged from 800 to 870 kJ/mol independently of the whisker orientation.

The above mechanical analysis shows that the whisker orientation effect lies only in the preexponential factor $\dot{\varepsilon}_e$ of the creep rate equation.

3.2 Structural study

3.2.1 Macroscopic observations

These concern the deformation anisotropy and the cavity nucleation at the sample scale. After deformation the sample shape was dependent on whisker orientation. Whereas the increase in cross-sectional area of S// specimens was more or less uniform, that of S⊥ samples presented a pronounced anisotropy. Strain in a direction parallel to the initial h-p.d. (i.e. in a direction perpendicular to the whisker planes) was systematically about twice that in a perpendicular direction. One of the goals of the TEM study was then to relate that observation to whisker and alumina-phase behaviours during deformation.

The deformation-induced porosity was estimated by density measurements in alcohol using Archimedes' principle. The loss in density never exceeded 4% in samples strained at about 90% and ranged typically from 0·5 to 2% for strains lower than 40%, depending on stress and temperature conditions, but not on specimen orientation, stress and temperature having opposite effects on density changes.

3.2.2 TEM observations

The microstructural study was focused on three main objectives: the general development of the specimen microstructure, the cavity formation and the particular role of whiskers.

From a general viewpoint, microstructural changes in strained samples were clearly visible at the TEM scale. They were mainly related to alumina grain growth and grain shape changes but never to structural changes due to some amorphous films

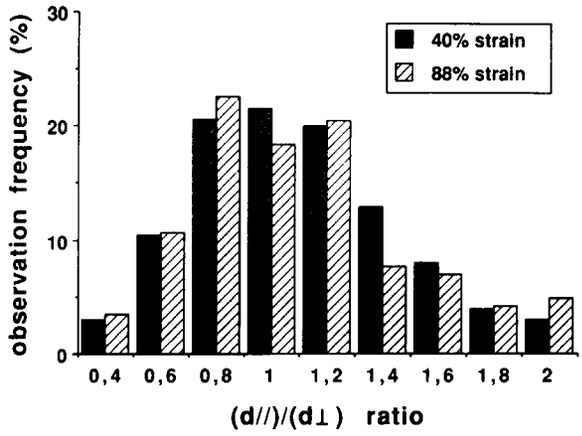

Fig. 4. Distribution function of the grain size ratio, $d//$h-p.d. over $d\perp$h-p.d., in a plane perpendicular to the stress axis in S⊥ specimens strained up to 40 and 88% at 1400°C.

developed at the interfaces during the tests. In the planes perpendicular to the compression axis, the average grain size, even larger than the initial one, was independent of the measurement direction in the two kinds of tested specimens S// or S⊥. As an example, Fig. 4 presents two histograms of the observation frequency of the ratio $d//$h-p.d. over $d\perp$h-p.d. ($d//$h-p.d. being the mean grain size in a direction parallel to the h-p.d. and $d\perp$h-p.d. that in a direction perpendicular to the h-p.d.) for two S⊥ specimens strained up to 40 and 88% respectively. On the other hand, in the planes parallel to stress, grains were elongated perpendicularly to the stress direction (Fig. 5), especially in the most strained samples, a feature already mentioned in alumina matrix[3] or in alumina-based materials.[13] The ratio between the respective grain sizes in the directions perpendicular and parallel to stress was found to be 1·6 for the maximum strains (88%). This means that the deformation due to grain boundary sliding

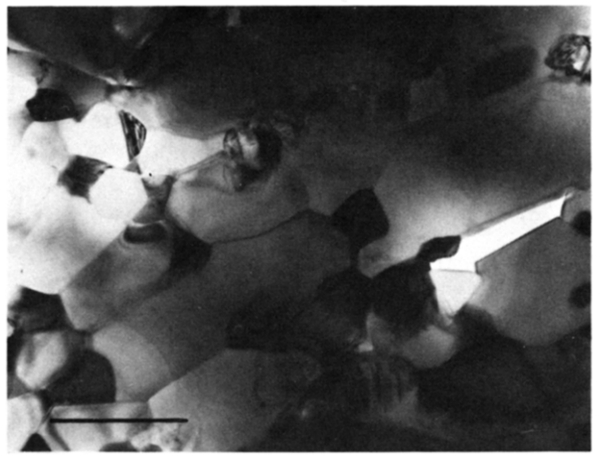

Fig. 5. Electron micrograph of S⊥ specimen strained up to 88% at 1400°C under 50 MPa; the arrow is parallel to the compression axis. Scale bar = 1 μm.

Fig. 6. Dislocations and zirconia particles in a large alumina grain. $\varepsilon = 40\%$, $T = 1400$°C, $\sigma = 50$ MPa Scale bar = 0·5 μm.

represented about 70% of the total strain in the creep experiments.[4]

Observation of dislocations in strained samples was an uncommon feature except in the largest grains inside which a lot of dislocations, gathered or not in subgrain boundaries, were observed (Fig. 6). Generally these grains contained zirconia particles which were already bound to boundaries by dislocations in the unstrained samples.[12] Multiplication of these dislocations during deformation tests is likely. However, the stresses that were applied in this work were not high enough to produce a generalized basal slip,[14] the easiest glide in sapphire, in the whole sample and under these conditions the dislocation plasticity cannot fully explain the large strains obtained in this work.

Cavities connected with the decrease in density never led to crack initiation and to sample fracture. These cavities generally had a small size and often a rounded shape like that associated with diffusion growth mechanisms and were often located on boundaries between alumina grains and SiC whiskers (Fig. 7). Their size never exceeded the size of adjacent grains. When they were elongated along a grain boundary, the growing direction was preferentially parallel to the stress axis at low strain, in agreement with the planes of maximum tensile stress but were randomly located on boundaries inclined at various orientations with respect to the compression axis at high strain (Fig. 8).

The rotational movement of whiskers relative to the stress direction was analysed by measuring on TEM micrographs the angle between whiskers and the compression axis. For the S// specimens that question was aimless, whiskers lying in planes perpendicular to the compression axis. On the other hand, in the case of S⊥ samples, it was found that (i) for the most part, whiskers still remained in planes

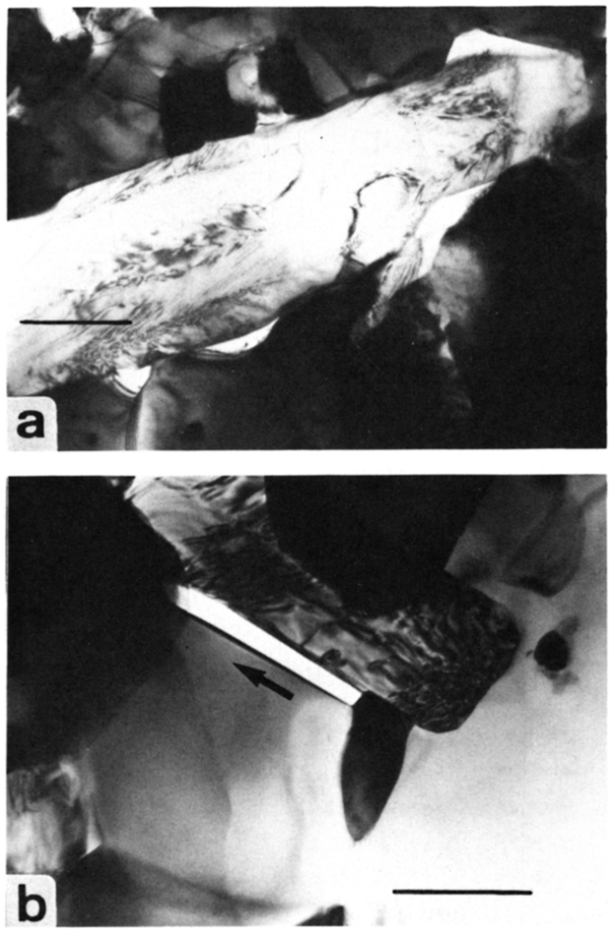

Fig. 7. Microstructure of strained samples showing cavities nucleated at alumina–SiC interfaces. The arrow is parallel to the stress direction. (a) Equilibrium shape, $\varepsilon = 12\%$, $T = 1350°C$, $\sigma = 64$ MPa. Scale bar = 1 μm. (b) Crack-like cavity, $\varepsilon = 10\%$, $T = 1350°C$, $\sigma = 64$ MPa. Scale bar = 0·5 μm.

perpendicular to the initial h-p.d. and (ii) they rotated in these planes so that the angle between the whiskers and the stress direction increased. From a nearly isotropic distribution at the creep test onset, the distribution curves for two specimens strained

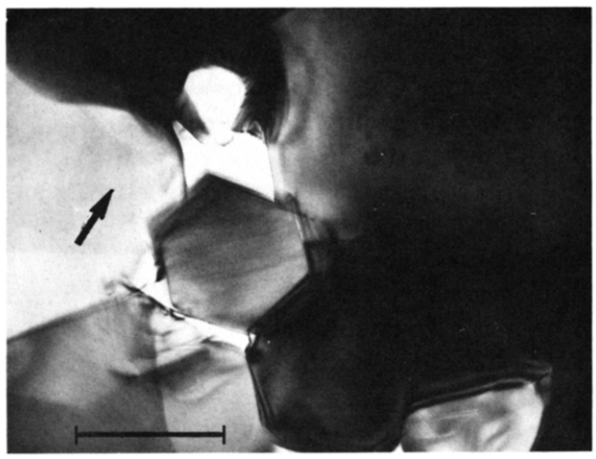

Fig. 8. Cavity at SiC interfaces with a random orientation. $\varepsilon = 60\%$, $T = 1400°C$, $\sigma = 50$ MPa. Scale bar = 0·5 μm. The compression axis is parallel to the arrow.

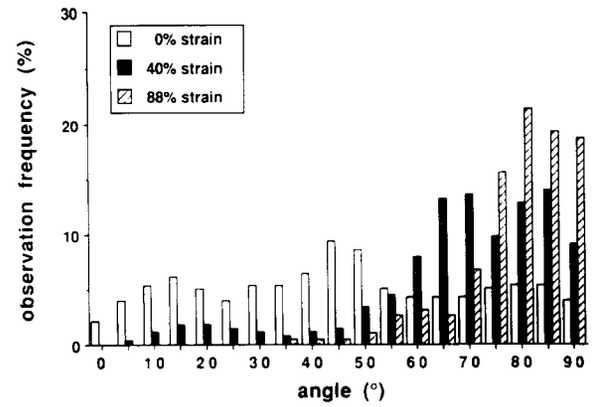

Fig. 9. Distribution function of the angle between the whisker direction and the stress axis in S⊥ specimens for three strain values: 0, 40 and 88% ($T = 1400°C$).

up to 40 and 88% respectively, are shown in Fig. 9. The whisker rotation clearly appears, the mean angle with compression axis being about 60° and 85° for the two strains. This means that deformation tended to align the whiskers in a direction perpendicular to the compression axis, a behaviour similar to that occurring during hot-pressing. The result was a more or less unidirectional alignment of whiskers, contrary to the initial distribution in the planes perpendicular to the h-p.d.

4 Discussion

The macroscopic mechanical behaviour showed that the influence of whisker orientation was only sensitive on the preexponential factor of the creep equation and on the deformation anisotropy, the other parameters (stress exponent, activation energy, threshold stress and creep damage) being nearly independent of whisker orientation. These results suggest that the deformation mechanisms are likely to be identical whatever the whisker orientation, i.e. diffusion-controlled boundary sliding.

The alumina–zirconia matrix can be considered as a soft one and the SiC whiskers as rigid inclusions which do not contribute to deformation. The preexponential factor of the creep relation must then reflect how the matrix flows according to whisker orientation, i.e. how the matrix and whiskers interact. The mechanical interaction between a soft matrix and rigid inclusions is poorly documented. A recent study by Yoon & Chen,[7] concerning a zirconia matrix containing mullite inclusions, has emphasized the influence of the shape and the volume fraction V of inclusions on the prefactor. In their paper, these authors considered that the interaction between the matrix and inclusions was only a mechanical one and the creep rate of the

matrix was represented by the usual power law $\dot{\varepsilon} = \alpha(\sigma/\sigma_0)^n$. The creep rate of the composite was then estimated by calculating the average stress remaining in the matrix by analogy with the flow of a newtonian fluid containing dilute rigid spherical inclusions. The stress concentration factor of each inclusion was found to be dependent only on the stress exponent of the matrix creep equation and the inclusion shape. When fibres are perpendicular to a tensile stress direction, the effect on the creep rate is similar to that resulting from addition of spherical inclusions, and the composite creep rate can be expressed as:

$$\dot{\varepsilon}\perp = (1 - V)^{2+n/2}\alpha(\Sigma/\sigma_0)^n \qquad (3)$$

where Σ is the macroscopic stress.

When the fibres are parallel to the tensile stress direction a shear stress at the fibre–matrix interface which transfers a load from the matrix to the fibre must be taken into consideration and the creep rate is then written as:

$$\dot{\varepsilon}// = (1 - V)^{1+(1+n/2)(L/R)}\alpha(\Sigma/\sigma_0)^n \qquad (4)$$

with L the half length and R the radius of the fibres.

According to the theory of Yoon & Chen, these results are valid for both tensile and compressive creep tests. Under these conditions, by taking $V = 0{\cdot}267$, $n = 1{\cdot}4$ and an average value of 4 for L/R, a creep rate ratio $\dot{\varepsilon}_{S\perp}/\dot{\varepsilon}_{S//}$ equal to 0·6 should be obtained, if $\dot{\varepsilon}_{S//}$ is approximated to $\dot{\varepsilon}\perp$ and $\dot{\varepsilon}_{S\perp}$ to 0·5 $(\dot{\varepsilon}// + \dot{\varepsilon}\perp)$, by taking into consideration the nearly isotropic distribution of whiskers in planes parallel to the compression axis in these specimens. Moreover, whatever the n value, the above ratio is always smaller than one. The present experimental values of the ratio, about 4, are inconsistent with that theory.

As a matter of fact the continuum theory of Yoon & Chen is mainly based on estimations of stress concentrations in the inclusions; tensile and compressive tests are equivalent. In the opinion of the present authors, it is not the stress direction relative to that of whiskers that must be considered, but rather the macroscopic direction of grain flows with respect to whisker axes. Plastic deformation tests correspond to flow conditions not to static ones. Under these conditions the behaviour of compressive samples containing whiskers perpendicular to the stress direction should be similar to that of tensile specimens inside which whiskers are nearly parallel to the stress direction. Indeed, these two different configurations correspond to equilibrium configurations inasmuch as whiskers tend to keep, during deformation, the same orientation relative to the stress direction in these two cases.

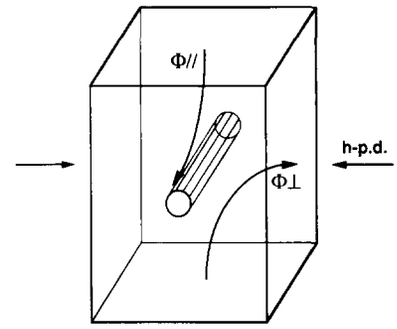

Fig. 10. Schematic drawing of flows around a whisker perpendicular to the vertical compression axis.

Considering these remarks, the creep rate when a whisker is perpendicular to the compression axis is now analysed. Two contributions may be distinguished (Fig. 10):

(i) A first one, where matter is removed from sample ends and deposed on the two sides parallel to the h-p.d.; let $\dot{E}//$ be the related creep rate, grain flow being partially parallel to the whisker; and

(ii) a second one, where the matter removed from the ends is added to the two faces perpendicular to the h-p.d. The grain flow is now perpendicular to the whisker; let $\dot{E}\perp$ be the corresponding creep rate.

According to whether the two kinds of flow are independent or not, two possibilities exist for the net creep rate calculation. In the S⊥ samples, when at the end of the creep tests the whiskers were nearly perpendicular to both the stress direction and the h-p.d., the two flows are nearly independent and act in parallel; the sample creep rate is therefore:

$$\dot{\varepsilon}_{S\perp} = \dot{E}// + \dot{E}\perp \qquad (5)$$

On the other hand, owing to the isotropic distribution of whiskers in planes perpendicular to the stress direction and the need to maintain the compatibility of local strains, the two flows are coupled in S// specimens. The resultant creep rate $\dot{\varepsilon}_{S//}$ is then controlled by the slowest of the two contributing rates and due to the shape anistropy of strained S⊥ samples leading to $\dot{E}\perp > \dot{E}//$, $\dot{\varepsilon}_{S//}$ can be roughly approximated to $\dot{E}//$.

The net creep rate ratio for the two kinds of specimens in the above conditions can then be written as:

$$\dot{\varepsilon}_{S\perp}/\dot{\varepsilon}_{S//} \approx (\dot{E}// + \dot{E}\perp)/\dot{E}// \qquad (6)$$

leading to $\dot{E}\perp \approx 3\dot{E}//$, by considering the experimental value of the creep rate ratio approximately equal to 4.

This value of $\dot{E}\perp/\dot{E}//$ is in good agreement with

that determined from strained S⊥ sample anisotropy, i.e. 2, by assuming that strains in the directions perpendicular or parallel to the h-p.d. are linearly related to the corresponding rates $\dot{E}\perp$ and $\dot{E}//$. The discrepancy is not significant, due to the simpleness of the hypotheses.

The net creep rate difference between samples containing whiskers perpendicular to the compression axis, S// specimens, and S⊥ ones at the end of creep tests, simply due to different whisker distributions, shows that the angle between the whisker axis and the stress direction is not an adequate criterion to account for the resultant creep rate.

The anisotropy of strained S⊥ samples, i.e. the disparity between $\dot{E}\perp$ and $\dot{E}//$, is likely to result from a greater ease of grain intercalation mechanisms when the whisker axis is perpendicular to the flow direction. The cross-sectional area of whiskers is then more favourable to that mechanism than the elongated longitudinal section.

These various results, creep rates and sample shapes according to the whisker orientation relative to the compression axis and to the h-p.d. are firstly in good agreement and secondly show that grain flows are easier when whiskers are oriented perpendicularly to these flows.

Now, concerning the threshold stress, its insensibility to whisker orientation excludes as a possible origin stresses due to differential thermal expansion between whiskers and the surrounding alumina matrix. Indeed, the thermal expansion coefficient of SiC whiskers being lower than that of alumina ($4{\cdot}7 \times 10^{-6}$ against $8{\cdot}6 \times 10^{-6}/^{\circ}C$), hoop and axial tensile stresses and radial compressive stresses should exist in the matrix at the test temperatures. According to the whisker orientation relative to the compression axis the effect of these possible stresses on creep rate is different. Schematically, when whiskers are parallel to the compression axis, axial stresses in the matrix are opposed to the applied stress; the observation of a threshold stress would be plausible in this case. On the other hand, when whiskers are perpendicular to the compression axis, thermal stresses tend to produce in the matrix a strain of the same sign as that resulting from the applied stress. The occurrence of a threshold stress under these conditions is anomalous and is not in agreement with the observations. The most likely conclusion is that, due to the high test temperatures, thermal stresses are relaxed, an hypothesis already advanced by other authors.[15]

The observation of a preferential pore nucleation at alumina–whisker interfaces is not surprising. When a stress is applied to a polycrystal, stress singularities and high local tensile stresses in the vicinity of triple junctions can be relaxed by matter diffusion from or to adjacent boundaries. Stress relaxation mechanisms involve appreciable grain boundary diffusion. If significant stress concentrations produced by grain boundary sliding are not expected in alumina,[16] on the other hand grain boundary diffusion in SiC is too slow ($D_b\delta_b = 2 \times 10^{-43}\,m^3/s$ for SiC at 1400°C[17] against $3 \times 10^{-22}\,m^3/s$ for Al_2O_3) to contribute to stress relaxation. Stress concentrations were then only reduced by matter diffusion in the alumina grains, thus reducing the efficiency of relaxation mechanisms. If grain boundary diffusion in alumina was fast enough to prevent a brittle intergranular fracture mode, cavity nucleation could nevertheless occur by vacancy coalescence in boundaries. This is the mode of boundary separation which was observed. From this viewpoint, alumina–SiC interfaces constituted places of weak strength in the composite.

According to observations up to about 25% strains, these cavities, once nucleated, either grew by retaining their equilibrium shape (Fig. 7(a)) or, if surface diffusion was too slow, by propagating along the interfaces nearly parallel to stress (Fig. 7(b)), along which tensile stresses had their maximum value. As deformation proceeded, cavity development was weak, showing that cavities were relatively stable, and the major difference resided in the random orientation of cavities.

This behaviour is not anomalous and as a point of fact reflects the elementary events, such as grain rotation and neighbour switching, that occur during superplastic deformation of a material containing grain boundary pores acting as a 'second phase', with the condition that those pores are stable. Similar results concerning the random orientation of porosity have been obtained by Crampon on magnesium oxide polycrystals[18] and by Chung & Davies[19] on uranium dioxide polycrystals containing 4% porosity. These last authors observed in their materials that the superplastic and non-superplastic behaviours were correlated to very different pore structures: rounded and randomly oriented pores in the first case and confined to boundaries parallel to the stress axis and showing large aspect ratios in the second case. Chung & Davies explained these observations from the model proposed by Ashby & Verrall[20] and by introducing stable pores at triple junctions.

One could object in the present case that owing to the absence of plasticity of the SiC phase the Ashby & Verrall model is not appropriate, this one needing

deformation of the four implied grains. The passage from the initial configuration to the final one in this model can be applied when one of the four grains is a rigid phase, by considering as possible that the rigid grain rotates under the effect of shear stresses acting on its boundaries.[21] Matter flows in the specimen are not uniform and flow velocity gradients can cause differential frictions that lead to rotation of the grains. That mechanism is similar to the one reorienting the whiskers away from the compression axis during deformation or hot-pressing. Under these conditions the observation of randomly oriented porosity is not inconsistent with the loading geometry.

5 Conclusions

Alumina–zirconia ceramics reinforced with SiC whiskers have been deformed during compressive creep tests up to large strains without sample fracture. The resultant porosity was weak and crack-like cavity length never exceeded the grain size. Superplastic deformation essentially resulted from diffusion mechanisms, dislocation observations being not able to account for the large strains obtained in this study.

The influence of whisker orientation relative to stress axis has been studied. Creep rate is dependent on that orientation but the angle between whisker and stress direction is not an adequate criterion. It is the direction of the matter flow in the whisker vicinity that must be considered; it appeared that the creep rate is larger when matter flow is perpendicular to the whisker axis. Creep rates and macroscopic shapes of strained samples are in agreement with that hypothesis.

Observation in this work of randomly oriented porosity in highly strained specimens supports the influence of elementary events on the superplastic deformation.

Finally the threshold stress is not related to thermal expansion anisotropy.

Acknowledgements

The authors would like to thank Céramiques Techniques Desmarquest who supplied the composite disk used in this study and the MRT for financial support. One of them (G. Bernard-Granger) is now a CIFRE research student at C.T. Desmarquest.

References

1. Carry, C. & Mocellin, A., Structural superplasticity in single-phase crystalline ceramics. *Ceram. Int.*, **13** (1987) 89–98.
2. Chen, I. W. & Xue, L. A., Development of superplastic structural ceramics. *J. Am. Ceram. Soc.*, **73** (1990) 2585–609.
3. Carry, C. & Mocellin, A., Superplastic forming of alumina. *Proc. Brit. Ceram. Soc.*, **33** (1983) 101–15.
4. Wakai, F., Kato, H., Sakaguchi, S. & Murayama, N., Compressive deformation of Y_2O_3-stabilized ZrO_2/Al_2O_3 composite. *Adv. Ceram. Mat.*, **3** (1988) 71–6.
5. Nieh, T. G., McNally, C. M. & Wadsworth, J., Superplastic behaviour of a 20% Al_2O_3/YTZ ceramic composite. *Scripta Metall.*, **23** (1989) 457–60.
6. Wakai, F., Kodoma, Y., Sakaguchi, S., Murayama, N., Izaki, K. & Nihara, K., A superplastic covalent crystal composite. *Nature*, **344** (1990) 421–3.
7. Yoon, C. K. & Chen, I. W., Superplastic flow of two-phase ceramics containing rigid inclusions: zirconia/mullite composites. *J. Am. Ceram. Soc.*, **73** (1990) 1655–65.
8. Nauer, M., Carry, C. & Duclos, R., Formage haute température de composites céramiques à matrice zircone renforcée par whiskers de SiC. In *Compte-rendus J.N.C.7*, ed. G. Fantozzi & P. Fleischmann. AMAC, Paris, 1990, pp. 421–31.
9. Duclos, R. & Crampon, J., Diffusional creep of a SiC whisker reinforced alumina/zirconia composite. *Scripta Metall. Mater.*, **23** (1989) 1673–8.
10. Arzt, E., Ashby, M. F. & Verrall, R. A., Interface controlled diffusional creep. *Acta Metall.*, **31** (1983) 1977–89.
11. Burton, B., Interface reaction-controlled diffusional creep. A consideration of grain boundary dislocation climb sources. *Mat. Sci. Eng.*, **10** (1972) 9–14.
12. Duclos, R., Crampon, J. & Cales, B., Microstructure development during hot-pressing of alumina-based ceramics reinforced with SiC whiskers. *Ceramics International*, **18** (1992) 57–63.
13. Martinez, R., Duclos, R. & Crampon, J., Structural evolution of a 20% ZrO_2/Al_2O_3 ceramic composite during superplastic deformation. *Scripta Metall. Mater.*, **24** (1990) 1979–84.
14. Heuer, A. H., Tighe, N. J. & Cannon, R. M., Plastic deformation of fined-grained alumina (Al_2O_3): II. Basal slip and nonaccommodated grain boundary sliding. *J. Am. Ceram. Soc.*, **63** (1980) 53–8.
15. Claussen, N., Weisskopf, K. L. & Rühle, M., Tetragonal zirconia polycrystals reinforced with SiC whiskers. *J. Am. Ceram. Soc.*, **69** (1986) 288–92.
16. Evans, A. G., Rice, J. R. & Hirth, J. P., Suppression of cavity formation in ceramics: prospect for superplasticity. *J. Am. Ceram. Soc.*, **63** (1980) 368–75.
17. Carry, C. & Mocellin, A., High temperature creep of dense fine grained silicon carbide. In *Deformation of ceramic materials II*, ed. R. E. Tressler & R. C. Bradt. Plenum Press, New York, 1984, pp. 391–404.
18. Crampon, J., The deformation microstructure and mechanisms of ultrafine-grained MgO at high temperature. In *Proc. 2nd Riso Int. Symp. Metall. Mater. Sci.*, ed. N. Hansen, A. Horsewell, T. Leffers & H. Lilholt. Riso Nat. Lab., Roskilde, Denmark, 1981, pp. 247–53.
19. Chung, T. E. & Davies, T. J., The superplastic creep of uranium dioxide. *J. Nucl. Mat.*, **79** (1979) 143–53.
20. Ashby, M. F. & Verrall, R. A., Diffusion accommodated flow and superplasticity. *Acta Metall.*, **21** (1973) 149–63.
21. Beeré, W., Stresses and deformation at grain boundaries. *Phil. Trans. Roy. Soc. London A*, **288** (1978) 177–96.